Open your mind. LUT.
Lappeenranta University of Technology

ENERGY SAVING POTENTIAL IN RESERVOIR PUMPING

Joni Siimesjärvi

Bachelor's thesis
LUT Energy
Electrical engineering

14.10.2014

ABSTRACT

Lappeenranta University of Technology
LUT School of Technology
LUT Institute of Energy Technology, Electrical Engineering

Joni Siimesjärvi
Energy saving potential in reservoir pumping

2014

Bachelor's Thesis.
34 p.

Examiner: D.Sc. Tero Ahonen

Pumping systems account for up to 22 % of the energy consumed by electrical motors in European industry. Many studies have shown that there is also a lot of potential for energy savings in these systems with the improvement of devices, flow control or surrounding system. The best method for more energy efficient pumping has to be found for each system separately.

This thesis studies how energy saving potential in reservoir pumping system is affected by surrounding variables, such as the static head variation and friction factor. The objective is to create generally applicable graphs to quickly compare methods for reducing pumping system's energy costs.

The gained results are several graphs showcasing how the chosen variables affect energy saving potential of the pumping system in one specific case. To judge if these graphs are generally applicable, more testing with different pumps and environments are required.

TIIVISTELMÄ

Lappeenrannan teknillinen yliopisto
Teknillinen tiedekunta
LUT Energia, sähkötekniikka

Joni Siimesjärvi
Energiansäästöpotentiaali säiliöpumppauksessa

2014

Kandidaatintyö.
34 s.

Tarkastaja: TkT Tero Ahonen

Pumppausjärjestelmät kuluttavat jopa 22 % sähkömoottoreiden kuluttamasta energiasta Euroopan teollisuudessa. Useat tutkimukset ovat todenneet, että näissä järjestelmissä on myös paljon energiansäästöpotentiaalia parantamalla laitteistoa, virtauksen ohjausta tai ympäröivää systeemiä. Paras tapa energiatehokkuuden saavuttamiseksi pitää löytää jokaiselle systeemille erikseen.

Tässä työssä tutkittiin miten energiansäästöpotentiaaliin säiliöpumppauksessa vaikuttavat ympäröivät muuttujat, kuten staattisen nostokorkeuden vaihtelu ja kitkakerroin. Tavoitteena on luoda yleisesti hyödynnettäviä kuvaajia, joilla voidaan nopeasti verrata tapoja vähentää pumppauksesta aiheutuvia energiakuluja.

Tuloksena saatiin useita kuvaajia, joista selviää miten valitut muuttujat vaikuttavat pumppausjärjestelmän energiasäästöpotentiaaliin yhdessä tapauksessa. Jotta voitaisiin arvioida ovatko nämä kuvaajat hyödynnettäviä yleisemmin, pitäisi suorittaa enemmän testejä eri pumpuilla erilaisissa ympäristöissä.

CONTENTS

ABBREVIATIONS AND SYMBOLS

rpm	Rounds per minute
VFD	Variable Frequency Drive

A	Area
C	Pump efficiency coefficient
g	Acceleration due to gravity
H	Head
K	Slope for speed ramp
k	Resistance coefficient
N	Rotational speed
P	Power
Q	Flow
S	Starting point for speed ramp
V	Volume

η	Efficiency
ρ	Density

Subscript

i	position of element in vector
max	maximum value
n	nominal value
p	value referred to pump curve
s	value referred to system curve
st	static
1	single value
2	single value

1. INTRODUCTION

In a world full of inefficient pumping, pumping systems account for almost 20 % of the world's electrical energy demand. A single industrial plant can have more than 50 % of its energy demand used in pumping systems. Examining already existing pumping systems and optimizing their usage is an enormous task, but it yields more significant results than focusing on the new systems. This is because there already exists such a large amount of pumping systems compared to what is built every year. During their lifetime pumping tasks may have changed, while no optimizing has been done for the pump or to its flow control method (Europump, 2001).

Selecting the most efficient solution to reduce pump's energy consumption is no simple matter. Various options come with different benefits and costs. Designing and installing new piping better optimized for the process can be very effective, but it usually comes with large costs that outweigh possible savings that could be gained in energy costs. In many cases retrofitting a variable frequency drive is considered to be a practical solution for more efficient pumping process (Ferman et al., 2008).

Pumps are often oversized for the sake of 'just to be on the safe side'. Pumps are sized so that they can deliver the maximum amount of flow demanded. On top of that for future expansion there has to be a reserve for even more flow. This practice causes pumps to run at non-optimal flows even when there is no significant variation in demanded flow rate. Therefore finding the best rotational speed for the current process can lead to large savings in energy costs, which can account for up to 40 % of pump's life cycle costs (Ferman et al., 2008).

In this thesis the research question is how surrounding variables affect the energy saving potential in a reservoir pumping system. The objective is to create graphs, which can be used to quickly determine difference in energy saving potential, when some parameters of the system are known. For this task a mathematical model is developed to simulate real-life pumps. Its validity is confirmed by comparing it with manufacturer's published characteristics and another mathematical model. Applying the developed model, pump's specific energy consumption is calculated considering changes in variables. Finally, graphs for energy saving potential in reservoir pumping system is formed from collected data.

After this introductory chapter, this thesis is primarily made out of four main chapters. Chapter two introduces the used system variables. In chapter three pump's mathematical model is found. Chapter four explains the theory and methods to gather data for graphs. In chapter five the acquired results are shown, analyzed and applied to a real life case.

2. RESERVOIR PUMPING SYSTEM

In a reservoir pumping system, fluid is pumped from one reservoir to another. This is very common in many water managing systems whether it is household water, drinking water or wastewater being pumped. Pumps in these systems are often driven at a constant speed without a variable frequency drive (VFD) able to adjust the pump speed to match the current demand. Since throttling has been used for a long time and it is a simple working method to regulate flow, other control methods can often be (without better knowledge) overlooked.

In this chapter a set of variables from pumping environment are chosen and their impact on energy saving potential of the pumping system is introduced. These variables are static head, resistance coefficient and flow control.

2.1 Static head

Static head H_{st} is defined by the height and pressure difference between fluid levels in reservoir pumping as seen in figure 2.1. This equals the initial pressure that pump has to overcome to deliver fluid to its destination when pumping fluid from a lower reservoir to higher one. Even though it is called static head, there is still variation in it due to pumping.

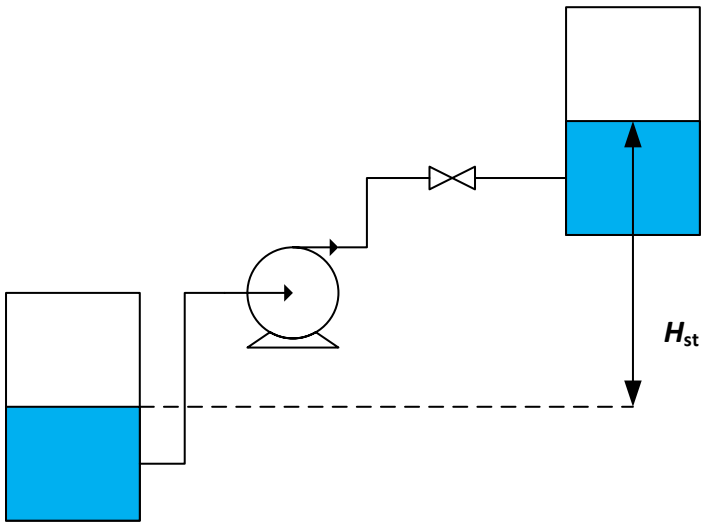

Figure 2.1 Static head H_{st} measured between reservoirs.

The amount of static head and its variation during pumping are the major factors when considering which flow control method to use to make a reservoir pumping system more energy efficient. Static head variation ΔH_{st} is measured as the difference of the maximum $H_{st,2}$ and the minimum $H_{st,1}$ values of static head as illustrated in figure 2.2. In a closed

loop system there is no static head as the liquid cycles through the system back to its starting point, and hence the height difference is zero.

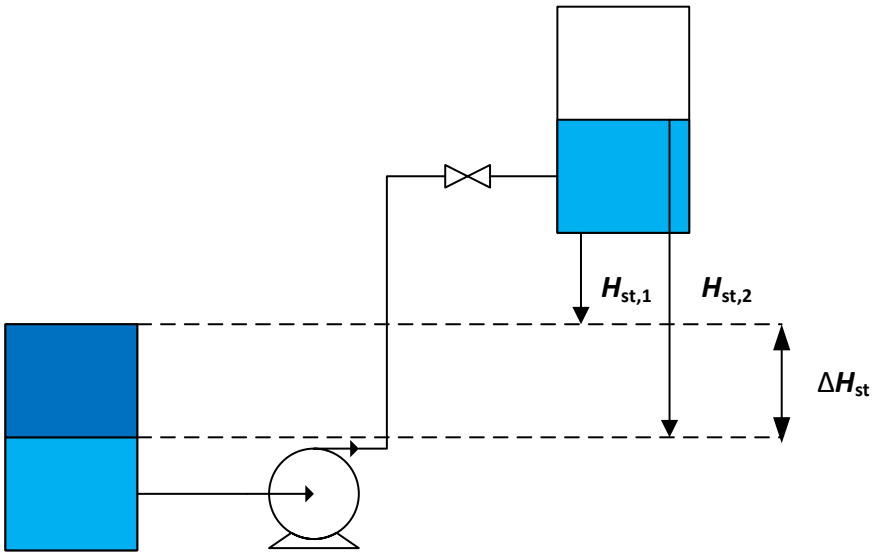

Figure 2.2 Static head variation due pumping. At the start of the pumping static head is $H_{st,1}$ and the higher reservoir is empty. During the pumping process the light blue fluid is transferred from lower reservoir to the higher one, and the static head is eventually $H_{st,2}$.

Due to the static head variation optimum rotational speed of the pump changes throughout the pumping process. This is illustrated in figure 2.3 for a pump with certain friction factor and static head variation. Increase in the static head increases specific energy consumption and also results in higher optimum rotational speed for the pump as seen in the figure.

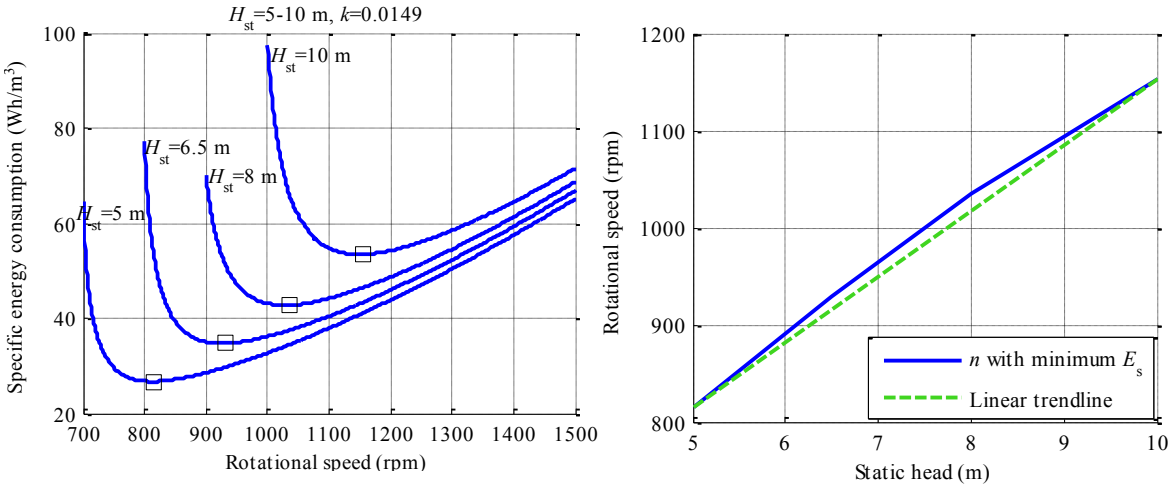

Figure 2.3 Optimum rotational speed of a pump affected by static head (Ahonen et al., 2014).

2.2 Resistance coefficient

Resistance coefficient gives the system its dynamic head. Unlike static head, dynamic head varies with the current flow rate according to the resistance coefficient.

Resistance coefficient is made up from friction losses in system. This includes roughness of the pipes, their length, diameter and material, possible valves and everything else that causes resistance to the fluid movement in the system. Since retrofitting piping is a costly operation, selection of resistance coefficient has to be correct when installing piping.

Total dynamic head of the system is made up from static head and dynamic head

$$H = H_{\mathrm{st}} + k * Q^2, \tag{2.1}$$

where H_{st} is static head, k is resistance coefficient and Q is volume flow rate. This equation (2.1) also provides the system curve of the process.

2.3 Flow control

Pumps are commonly sized to meet the maximum flow requirements while the pumping process does not necessarily always need that much flow. Controlling the flow is essential to gain demanded rates. This can be done by adjusting either the system curve or the pump curve accordingly so that the current operation point moves alongside the intersection of these two curves.

Valve throttling is a commonly used method to adjust the flow in a system. While achieving its purpose, this method is also inefficient. By throttling valves, one can adjust the system curve by increasing the amount of friction head loss. However this will make the pumping system operate less energy efficiently.

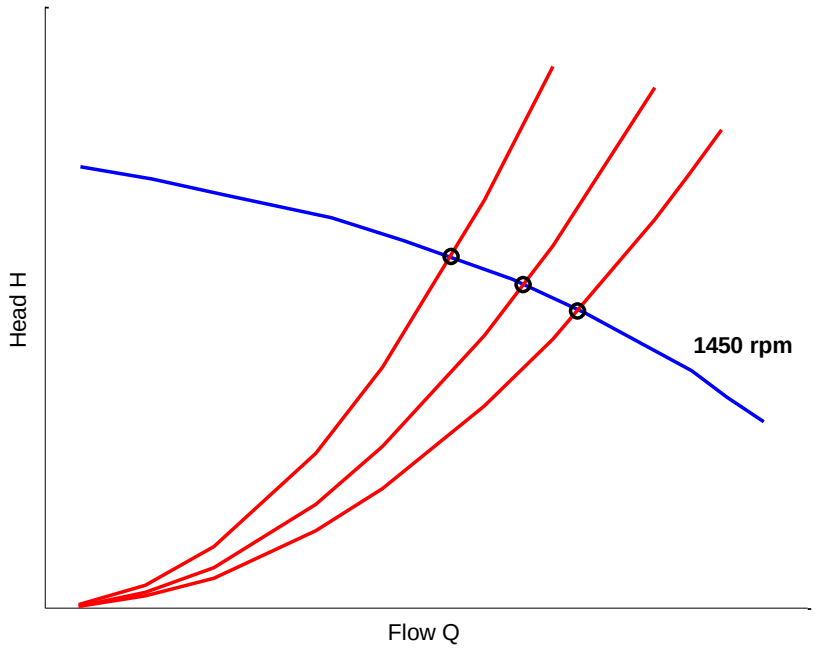

Figure 2.4 Effects of throttle control on system curve. Closing throttling valve causes the red system curve to be steeper. This moves the operation point and lower flow rates can be gained at the cost of increased head amount which results in larger energy consumption.

As an alternative, variable frequency drive can be used to adjust the pump curve. Changing shaft speed alters the pump curve, while the operation point moves alongside the intersection of the pump curve and the system curve. According to the affinity laws for pumps, pump power consumption can be proportional to the cube of shaft speed

$$\frac{P_1}{P_2} = \left(\frac{N_1}{N_2}\right)^3, \tag{2.2}$$

where P is power and N is rotational speed. Subscripts indicate corresponding power and rotational speed values. From this equation it can be concluded that even a slightly lower speed can have a notable impact in energy saving.

In systems that are dominated by static head, small change in the pump speed can have a huge impact on the flow rate. This is due to the smaller operation region on the system curve, as high static head brings it closer to the pump curve to begin with. Lowering the speed causes the operation point to quickly move close to shut-off head where there is no flow, but the pump is still running. Prolonged operation in this region can cause serious damage to pump's mechanics (Shields, 2004).

On the other hand systems dominated by friction head provide an excellent environment to fully utilize the benefits of VFD. As there is less static head, pump affinity laws are more accurate and give a better view on how much reducing shaft speed affects power.

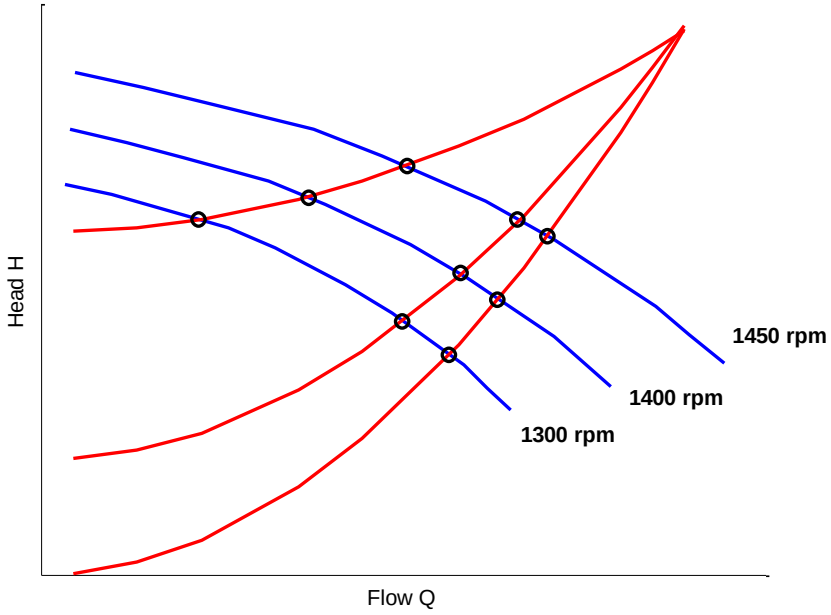

Figure 2.5 Effects of speed control on the pump curve. The bottom red curve is from system with no static head and the top red curve is from system with static head. Adding static head causes energy losses due to higher pressure that the pump has to overcome, to deliver the same amount of flow.

The effect on consumed specific energy is immense. In figure 2.6 specific energy consumption E_s (wh/m^3) is represented in each intersection of above figures for both VFD and throttle control. Values for VFD controlled system were taken from system curve with no static head. Effects of throttle control can be clearly seen. While VFD reduces specific energy consumption, throttle control increases consumption because of increased friction to the system.

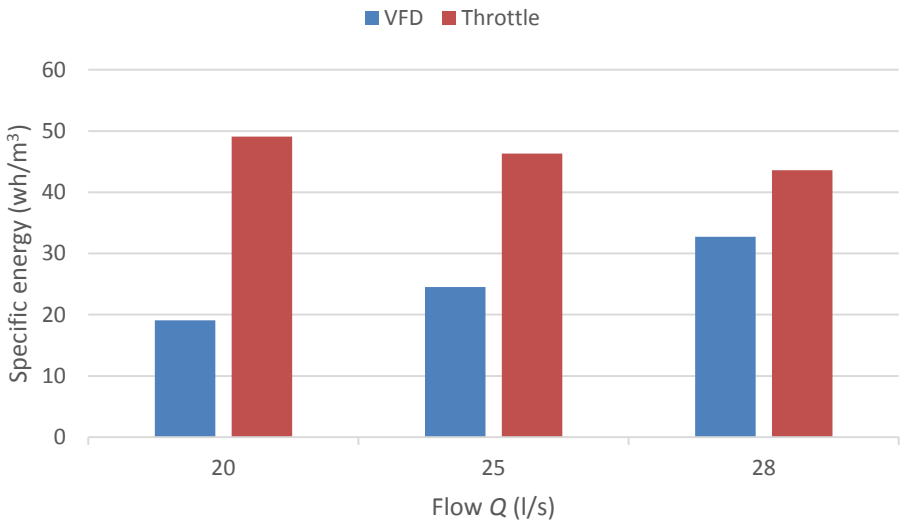

Figure 2.6 Specific energy consumption of VFD and throttle control.

Other means of flow control include changing the diameter of pump's impeller, replacing entire pump with one that has more suitable characteristics, bypass control, on-off -control or having multiple pumps in parallel or in series.

2.3.1 VFD-based flow control

From possible flow control methods, two were chosen for this study, speed ramp and the best constant speed. Both of the chosen control methods utilize VFD. These flow control methods were chosen since they were both efficient in energy and costs while also differ from one another enough that one could make arguments which to use for either case.

Speed ramp control method provides a slope which indicates the best speed for the pumping process based on the current amount of static head. This method was chosen since static head variation happens throughout the pumping process and it affects the best current rotational speed of the pump as seen in figure 2.3. As can be seen from the figure this correlation is not perfectly linear. To make calculations simpler it is considered to be linear. This flow control method heavily utilizes VFD and its possibilities (Ahonen et al., 2014). Commercial products for this control method were not found.

The best constant speed control method can be considered as a simplified version of the speed ramp. Finding this for the entire known pumping process is also a step in the right direction when optimizing pumping systems. As stated in chapter one, this method can be used in most cases to improve efficiency (Ruuskanen, 2007). Commercial application of the best constant speed method could be for example Flygt SmartRun which can find the best constant speed for the process when the static head variation is minimal. SmartRun

carries out reservoir drainage at a pre-select constant rotational speed. Depending on specific energy consumption either a higher or lower speed is chosen for the next drainage event and its effect on the system energy consumption is monitored (Ahonen et al., 2014).

3. PUMP MODEL

To accumulate data for this thesis, a general mathematical model for the pump is necessary. There has to be as few prerequisites as possible while still maintaining accuracy. This chapter introduces two developed models, which are compared with manufacturer's published data to see which of the models is used for the thesis.

3.1 ABB pump model

ABB Oy has created a PumpSave tool which calculates available energy savings when using ABB variable speed AC drives instead of other flow controlling systems. Their model requires pump's maximum delivery head H_{max}, nominal head H_n, nominal flow Q_n and the maximum pump efficiency to be known. The model gives a head value with the given flow

$$H_{\mathrm{i}} = H_{\mathrm{max}} - \left(\frac{Q_{\mathrm{i}}}{Q_{\mathrm{n}}}\right)^2 * (H_{\mathrm{max}} - H_{\mathrm{n}}), \tag{3.1}$$

where H_{i} is the head provided while the flow rate is Q_{i}. With a vector of flow values

$$\bar{Q} = [0.1, \dots, 1.5] * Q_{\mathrm{n}}, \tag{3.2}$$

pump's *QH* curve can be formed.

There is a coefficient for pump's efficiency at each given flow rate, assuming that motor efficiency always remains constant during the pumping process. As this thesis' primary focus is on pumps and motor efficiency varies on case by case basis, motor efficiency is neglected and left out of calculations. The coefficient given for the pump efficiency is defined based on ABB's own experience (ABB Oy, 2012)

$$C = \frac{Q_{\mathrm{i}} * \left(2.4 - 1.44 * \frac{Q_{\mathrm{i}}}{Q_{\mathrm{n}}}\right)}{Q_{\mathrm{n}}}. \tag{3.3}$$

However, accuracy of this coefficient decreases dramatically at higher flow rates since it is stated this coefficient works primarily on flow rates from 20 % to 100 % nominal (ABB Oy, 2012). Solution to this used in PumpSave is to keep the efficiency at the pump's maximum efficiency once it has been reached while moving towards the end of the curve.

Utilizing flow vector (3.2), a coefficient vector for pump efficiency can be calculated by using the equation (3.3). Multiplying this vector with the pump's best efficiency produces a vector containing efficiencies corresponding the given flow rates

$$\eta = \eta_{\max} * C. \tag{3.4}$$

With these values the shaft power of a pump can be calculated with equation

$$P_{\mathrm{i}} = \frac{\rho * g * Q_{\mathrm{i}} * H_{\mathrm{i}}}{\eta_{\mathrm{i}}}, \tag{3.5}$$

where ρ is the fluid density, g is the acceleration due to gravity and η_{i} is the pump efficiency.

3.2 Bene model

To have a better context whether or not ABB's model is accurate, another model was looked up. This model, from here on known as alternative model, was used in doctoral thesis handling pump schedule optimization (Bene, 2013). Instead of Q_{n} value, Bene model uses $Q_{\mathrm{ref.max}}$ which is assumed to be

$$Q_{\mathrm{ref.max}} = 2 * Q_{\mathrm{n}}. \tag{3.6}$$

The equation for pump's head resembles the one given by ABB with slight changes. It is stated that this equation is highly simplified and is only qualitatively similar to real performance curves

$$H_{\mathrm{i}} = H_{\max} * \left(1 - \left(\frac{Q_{\mathrm{i}}}{Q_{\mathrm{ref.max}}}\right)^2\right). \tag{3.7}$$

Efficiency is calculated assuming a constant maximum efficiency for the sake of simplicity

$$\eta_{\mathrm{i}} = 4 * \eta_{\max} * \left(1 - \frac{Q_{\mathrm{i}}}{Q_{\mathrm{ref.max}}}\right) * \frac{Q_{\mathrm{i}}}{Q_{\mathrm{ref.max}}}. \tag{3.8}$$

While power values are still calculated with (3.5), these equations provide sufficient basis for comparing this pump model with the ABB's one.

3.3 Accuracy

Models' accuracy is analyzed by comparing typical pump's characteristic curves with values gained from Sulzer APP 22-80 centrifugal pump, from here on referred to as Sulzer, in a specific pump laboratory environment shown in figure 3.1. The pump is being driven by an 11 kW ABB induction motor and an ABB ACS 800 frequency converter (Ahonen,

2011). The pump is connected to a system consisting of piping and control valves. This pumping environment is later used for simulating reservoir pumping system with known static head variation and friction factors.

Figure 3.1 Sulzer APP 22-80 pump in a pumping laboratory.

With the pump impeller diameter of 266 mm, figure 3.2 is used to gain manufacturer's *QH* curve for Sulzer.

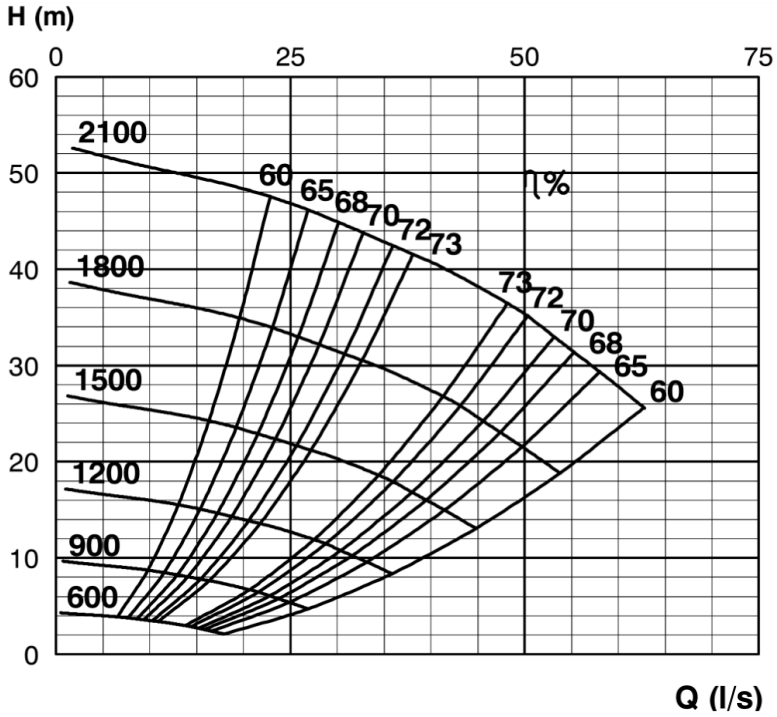

Figure 3.2 *QH* curves for various rotational speeds of APP 22-80.

Each model had the same flow values ranging from 10 % to 150 % of nominal adding 10 % for each operation point. Head and efficiency values were calculated with equations (3.1), (3.4), (3.7) and (3.8) for their respective models. Values for Sulzer were gained from manufacturer's characteristic curve shown in figure 3.2 by estimating head and flow values for curve with rotational speed of 1460 rpm.

QH curve is pump's performance curve also known as the pump curve. In figure 3.3 there are *QH* curves for the ABB model, alternative model and one provided by pump's manufacturer from here on referred to as original. Relative axes are based on their ratio compared to nominal values with 100 % being the nominal point. At flow rates less than nominal both models provide similar estimation to head value with margin of error at 6 % points at the flow rate of 40 %. With higher flow rates alternative model is giving better estimation.

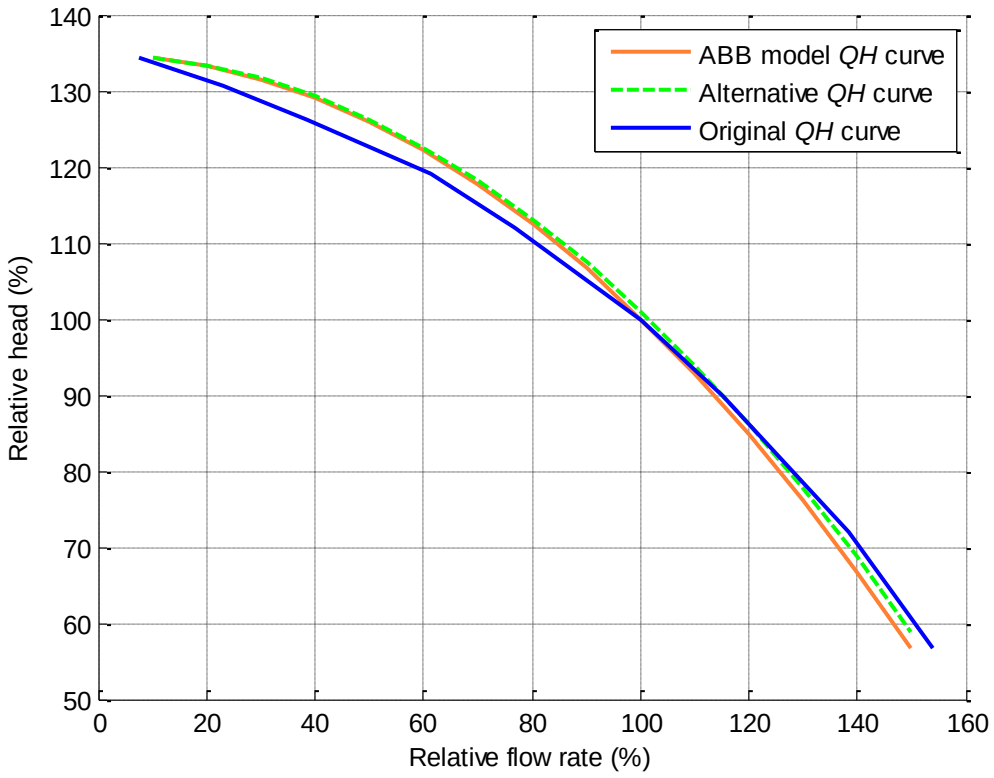

Figure 3.3 *QH* curves. Pump head models compared with manufacturer's curve.

Figure 3.4 has four $Q\eta$ curves. As a difference to figure 3.3, this figure also has curve for ABB's solution that keeps maximum pump efficiency after nominal point. This is later on referred to as ABB fixed curve. Axis with η resembles actual efficiency values while flow rates are still relative to the nominal flow.

After nominal point, original ABB model can have margin of error up to 30 % points in efficiency values when operating at flows over 150 %. While there is no need for such high flow values, even at 120 % nominal flow rate there is 12 % point difference in between the actual value and estimation. However with solution used in PumpSave tool that has fixed efficiency after achieving nominal flow, it appears that at 120 % nominal flow margin of error is 3 % points, which is lower than the absolute maximum margin of error of the entire curve which is at 4 % points.

The alternative model is more accurate when operating range is closer to the best efficiency point and includes higher than nominal values. However flow control usually focuses on reducing speed of the pump and therefore reducing flow rate and at the lower flow rates ABB model is more accurate.

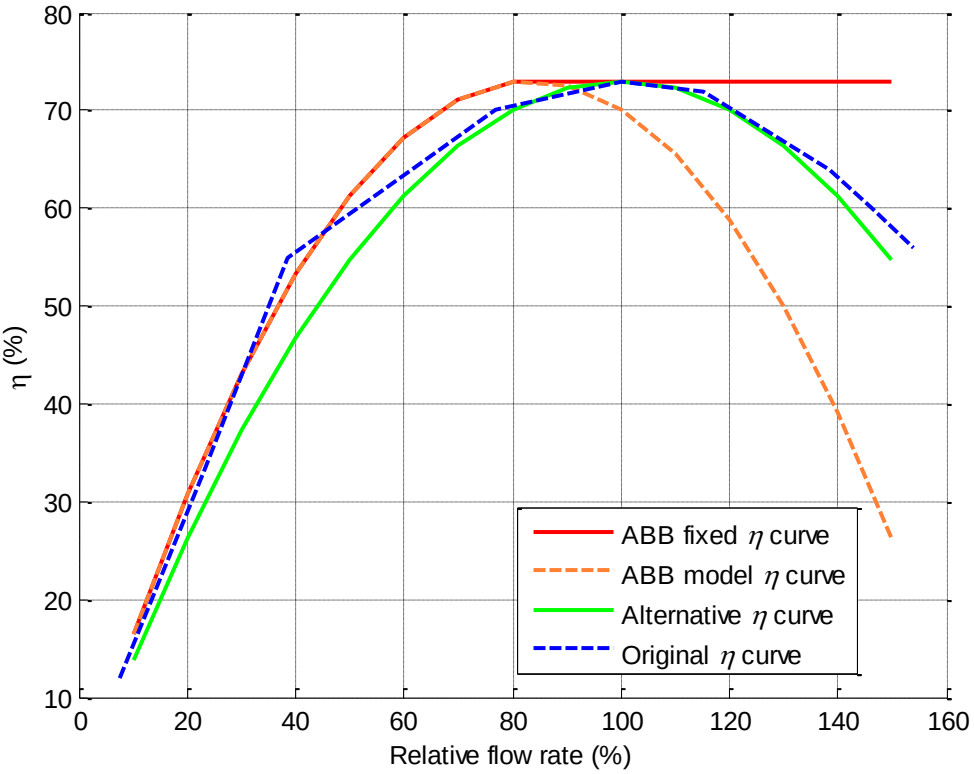

Figure 3.4 Qη curves. Models' efficiency curves compared to manufacturer's curve. Clearly the ABB model without fix is not accurate after the nominal point. ABB fixed curve is accurate up to 120 % flow rate. Alternative model's curve is not as precise when flow rate is between 20 % and 60 % but delivers the best accuracy after 100 % flow.

In figure 3.5 there are *QP* curves of each of the beforehand mentioned cases. These curves are the most important since they represent the accuracy of power consumption.

As seen in figure 3.4 efficiency for ABB model goes very low for higher flow rates which in turn causes power consumption to spike up. Hence this model can't be used in future calculations for graph data.

In both ABB's fixed curve and alternative curve there are areas where one's accuracy slips while the other maintains it. As previously mentioned, flow control usually reduces flow rate. From this fact it is decided that ABB's fixed model is being used as generalized pump model since it resembles the original curve more in lower flow regions unlike the alternative model. Up to the 110 % nominal flow, the fixed model is the most accurate one.

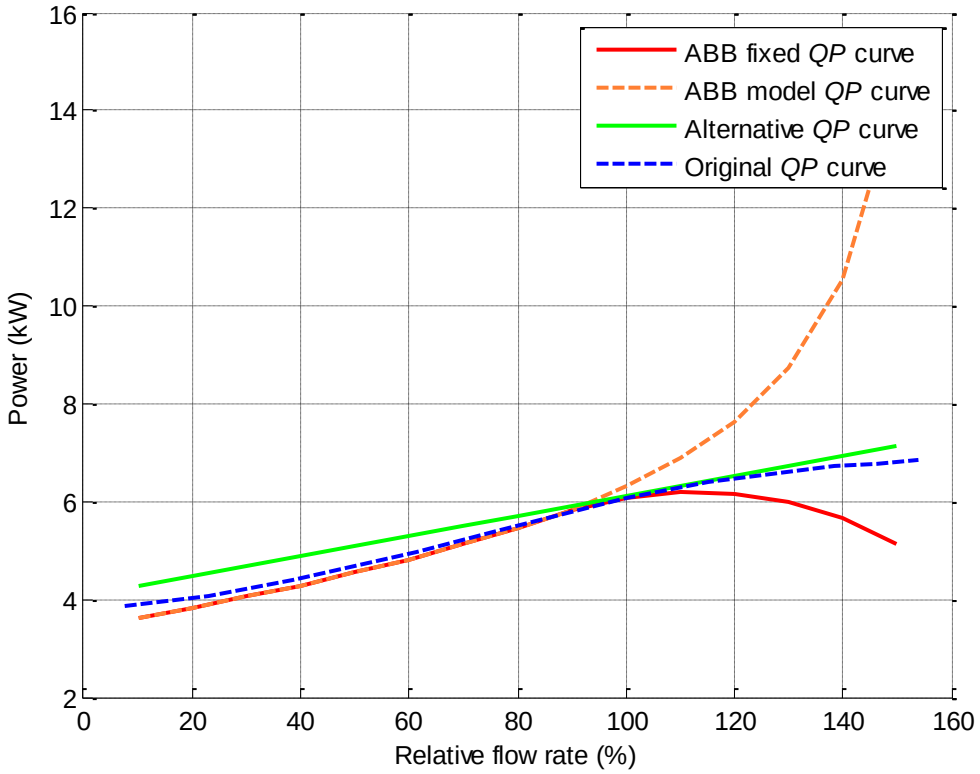

Figure 3.5 *QP* curves. Because of efficiency not being accurate for the ABB model after 100 % its estimation for power is way higher than the one provided by manufacturer's curve. The alternative model is the best one after 100 % flow but it is unreliable with lower than nominal flow rates. The ABB fixed curve is the most accurate if the flow rates do not exceed 120 % flow rate.

Finding a model that could combine the best areas from both ABB and alternative would create the most accurate results. In figures 3.6 and 3.7 it is illustrated how these models could work together. It would be tempting to blindly take advantages from these both cases to minimize downsides of model, but for the sake of continuity and cohesion this will not be the case. If in this thesis the operation region would be the entirety of above presented flow rates then usage of this combined model could be considered.

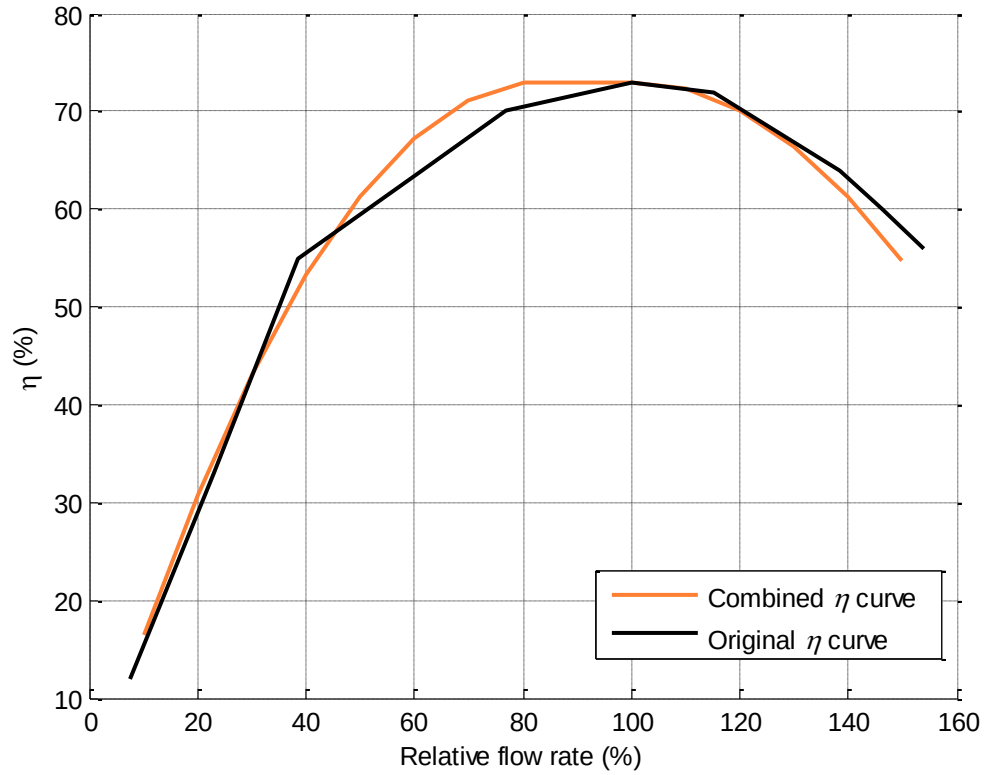

Figure 3.6 Combined η curve. Both the ABB model and the alternative model have their best areas combined.

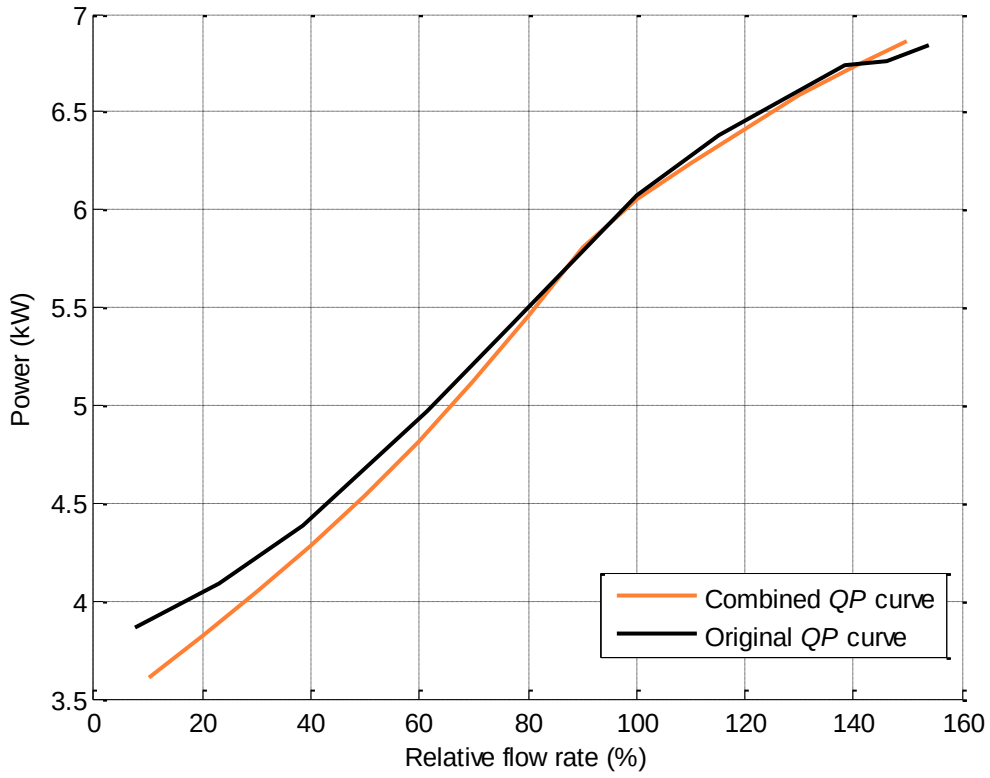

Figure 3.7 Combined *QP* curve. Results of the combined model's power estimation.

4. DATA GENERATING METHOD

Now that the model to be used is decided, ABB's fixed model, next step is to generate data for graphical analysis. First it is necessary to decide what the constant values for the pump and the process are. Since Sulzer pump was used to determinate accuracy of the models it is chosen to be used here also as our typical pump. For that pump maximum head is 22 m, nominal speed is 1450 rpm, nominal head is 16.3 m, nominal flow is 27.6 l/s and the best efficiency is 73 %. For the process it is approximated that base resistance coefficient *k* for used simulation is 0.0149 in this particular pump lab process environment (Ahonen et al., 2014).

As decided in chapter two, pump's VFD control methods for the flow rate are the speed ramp and the best constant speed. Calculating this data was divided into two functions using Matlab programming language. Both of these functions utilize same principles of calculating average specific energy consumption of the process for each case.

Pumping process is simulated so that static head rises in time discrete environment with one second time domain starting from the lowest point moving on to the highest, these points given to the above mentioned functions as parameters. Applying the selected pump model with above decided constants, the head, efficiency and power vectors are calculated from a vector of flows $\overline{Q_\mathrm{n}}$ containing values proportional to nominal value ranging from 10 % to 150 %.

The current operation point is calculated from intersection of the pump curve and the system curve. Affinity laws for pump are used to adjust the pump curve to the current rotational speed to get the correct flow and head values for the pump

$$\overline{Q_\mathrm{p}} = \overline{Q_\mathrm{n}} * \frac{N}{N_\mathrm{n}}, \tag{4.1}$$

$$\overline{H_\mathrm{p}} = \overline{H_\mathrm{n}} * \left(\frac{N}{N_\mathrm{n}}\right)^2. \tag{4.2}$$

These vectors contain values of pump curve with the new rotational speed *N*. System curve is made up from two vectors of *Q* and *H* values also. Vector $\overline{Q_\mathrm{s}}$ is made from values ranging from 0 to 150 % nominal with subtracted 1 from the end so the range does not exceed pump's operating range by any chance. From equation (2.1) vector for head values is calculated

$$\overline{H_\mathrm{s}} = H_\mathrm{st} + k * \overline{Q_\mathrm{s}}^2. \tag{4.3}$$

These four vectors make for system and pump curve. With `intersections` function, operation point can be calculated in the current circumstances. It should be noted that instead of current flow Q this function returns current volume V because of time discrete simulation process. This volume is stored for later to be used on specific energy calculation.

Power at the current V value is found with `interp1` function of Matlab using shape-preserving piecewise cubic interpolation method. This value is also stored for later calculations. As for parameters to the function there are current volume V_{current}, adjusted flow $\overline{Q_{\text{p}}}$ and power $\overline{P_{\text{p}}}$ adjusted with affinity laws

$$\overline{P_{\text{p}}} = \overline{P_{\text{n}}} * \left(\frac{N}{N_{\text{n}}}\right)^3. \tag{4.4}$$

This power calculation does not take into account changes in pump efficiency due to speed variation. Next a new value for static head is calculated with

$$H_{\text{st,new}} = H_{\text{st,current}} + \frac{V_{\text{current}}}{A}, \tag{4.5}$$

where A is area of the reservoir and V_{current} is current volume of the fluid. In this case area is 0.75 m^2 as this is the area of reservoir in Sulzer's pumping process. This procedure is repeated until H_{st} has reached the predetermined highest value.

After this is done, the average specific energy consumption of the process can be calculated with following equation (Europump, 2004)

$$E_{\text{s}} = \frac{E}{V}. \tag{4.6}$$

For this, total energy and volume are calculated from gathered data with numerical integration using trapezoidal method.

Function for constant speed `generate_const_data` starts off by calculating best constant speed for the eventual top value of static head $H_{\text{st,2}}$ by comparing specific energy consumed in pumping process with different speed values. Resolution for the speed values was set to 5 rpm. Then same process is repeated for starting value of static head $H_{\text{st,1}}$. Now that the best constant speed is determined for both beginning and the end of process, it is assumed that the best constant speed for the entire process is somewhere between these two values. Pump's rotational speed is increased from the lowest speed until the highest speed

has been reached, while calculating specific energy for each case into a matrix. Now from this matrix the lowest specific energy value is found and can be compared to specific energy used by the same process if it was done with nominal speed of 1450 rpm.

Function for the speed ramp `generate_ramp_data` uses same calculations for the best constant speed for both starting and ending values of static head. From these values a slope *K* can be calculated (Ahonen et al., 2014) for the speed ramp

$$K = \frac{N_{\mathrm{opt2}} - N_{\mathrm{opt1}}}{H_{\mathrm{st2}} - H_{\mathrm{st1}}}, \tag{4.7}$$

where N_{opt2} is optimal speed for the highest static head H_{st2} and N_{opt1} is optimal speed for the lowest static head H_{st1}. To complete this function for speed ramp, its starting point *S* has to be calculated. This can be done with a simple equation now that *K* value is known

$$S = N_{\mathrm{opt1}} - K * H_{\mathrm{st1}}. \tag{4.8}$$

It should be noted that any known static head and corresponding optimum speed value could be used to calculate *S*. The entire function for speed ramp then gets its final form

$$N_{\mathrm{current}} = S + K * H_{\mathrm{st,current}}. \tag{4.9}$$

Now specific energy can be calculated with speed that is dependent on amount of current static head.

In figure 4.1 the entire calculation process is presented as a block diagram. Both of the functions for flow control methods are explained step by step. Each time there is mention about specific energy calculation in one of the steps of the functions, it is a reference to the diagram next to them showing how the equations of this chapter have been used to calculate specific energy.

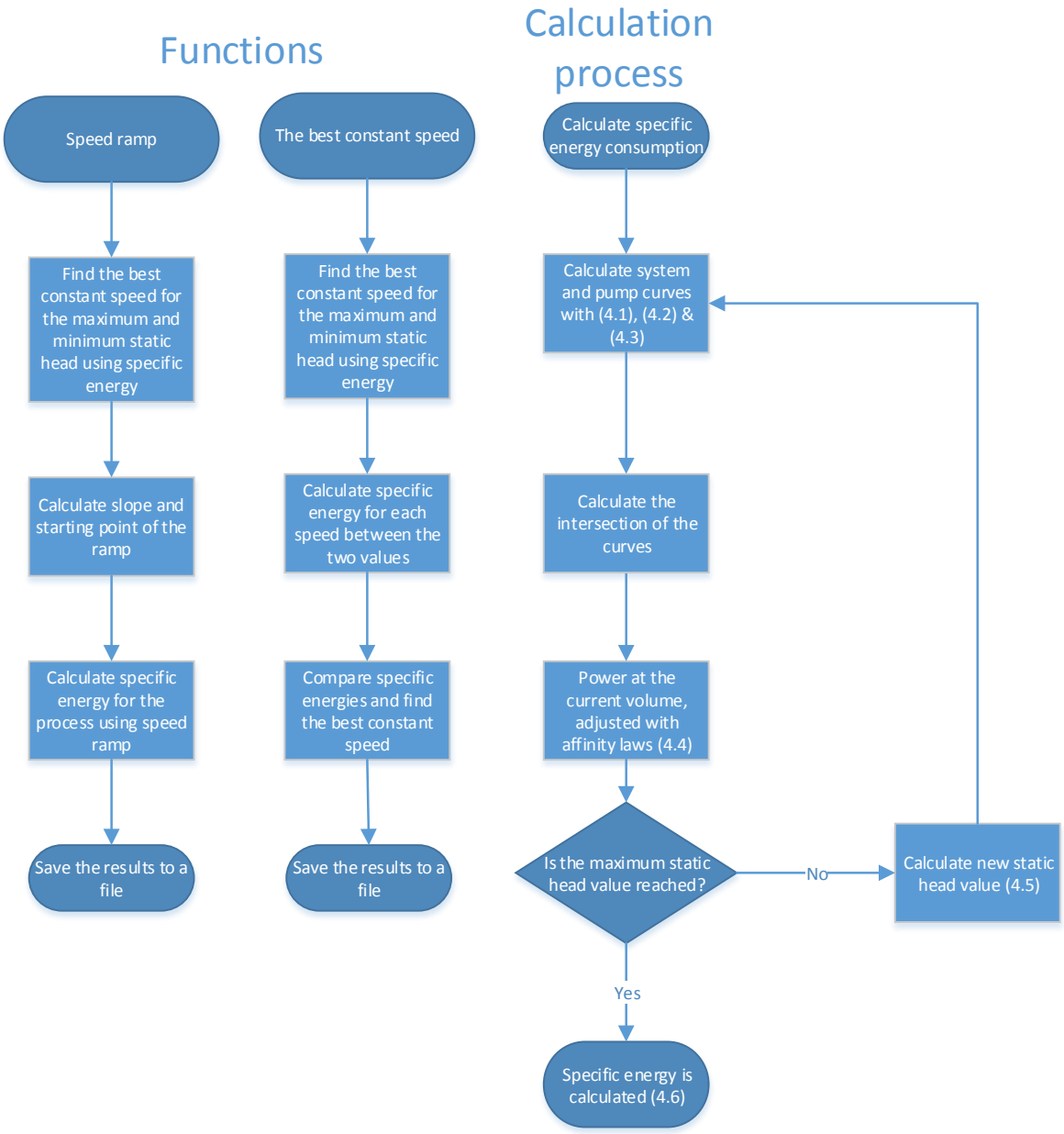

Figure 4.1 Block diagram of the calculation process. Procedure of both the best constant speed and the speed ramp functions and how they calculate specific energy consumption.

5. RESULTS

In this chapter the resulting energy saving potential graphs are presented and analyzed. After analyzing the graphs, they are applied to a real life case to make an example of their usage.

5.1 Comparison of VFD-based control methods

In figure 5.1, energy saving potential with the use of variable speed operation is shown when the system was operated with base value k_{base} for friction factor. In the first plot the best constant speed control has been used, and in the second plot speed ramp has been used. Both plots have three curves for different static head variations. Comparing both plots it seems that when static head variation $\Delta H_{st}/H_{max}$ is less than 0.1, then there is only little difference within savings gained from either control method. On the other hand, higher variation of 0.4 can cause up to 10 % point difference in saving potential between the two methods. When saving potential reaches zero it means that operating the system with fixed speed of 1450 rpm, the nominal speed of the pump, is a good solution.

For both control methods, decrease of static head amount H_{st}/H_{max} is increasing the amount of potential energy savings. This static head amount is calculated by comparing the highest static head value to the maximum head that the pump can provide.

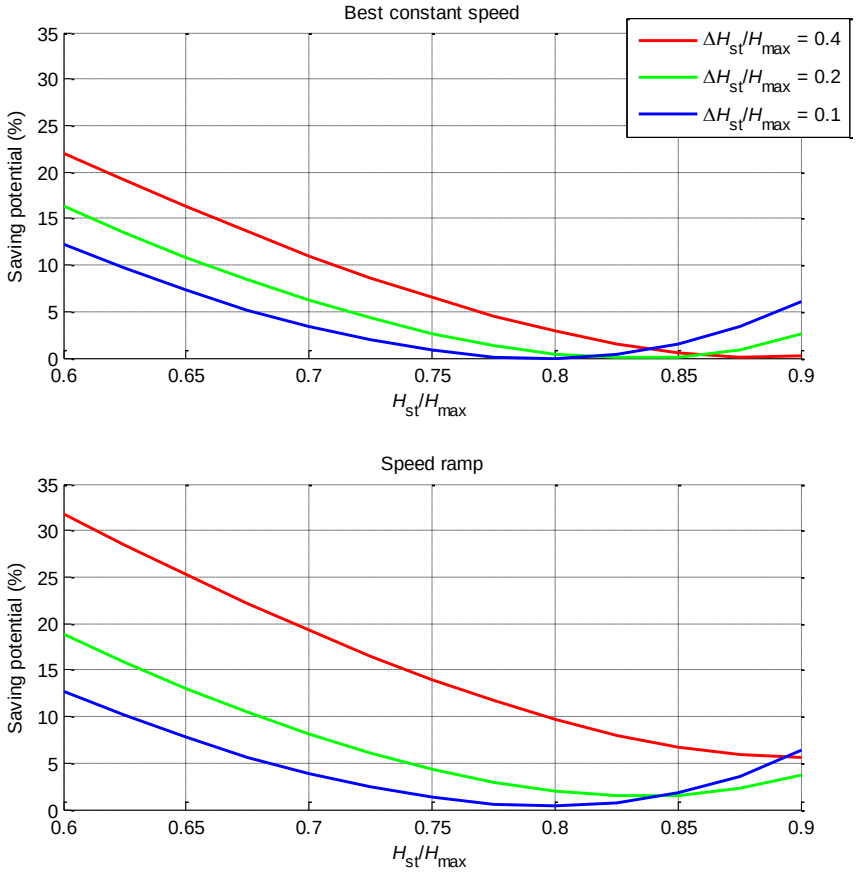

Figure 5.1 Saving potential with two control methods using base simulation value for friction factor k_{base}.

Comparison between speed ramp and constant nominal rotational speed of 1450 rpm in figure 5.2 shows how much less specific energy is consumed in same process using the speed ramp. Highest potential savings are gained from systems with relatively low static head compared to maximum head that can be provided by pump. Also more variation in static head during the process naturally means that there is more room to benefit from a speed ramp. This leads to a higher energy saving potential. The "green area" with no savings potential is operation region where constant speed of 1450 rpm is a good solution for the process.

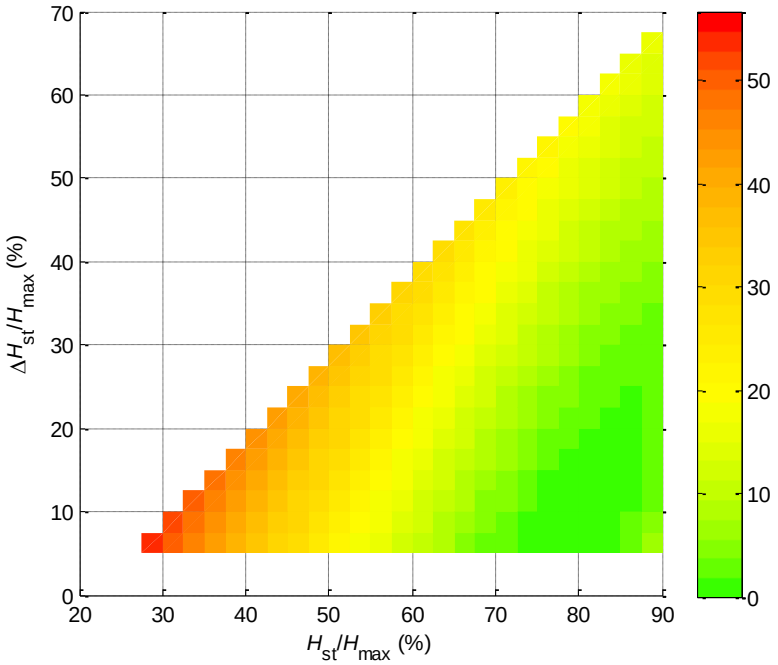

Figure 5.2 Speed ramp compared to nominal rotational speed of 1450 rpm (%).

Figure 5.3 has comparison between the best constant speed and constant nominal rotational speed of 1450 rpm. Like in previous figure, figure 5.3 has highest saving potential in systems with little relative static head. It is practically identical in that area. On the other hand, increased variation of static head does not provide nearly as much energy savings as with the other method when the variation in the pumping system is over 0.4. There can be seen a slight increase in saving potential on the bottom right corners of figures 5.2 and 5.3 where static head variation is less than 0.1 and the amount of static compared to maximum head is 0.9. This is an area where the pump operation point exceeds the nominal, but not by a large margin. It seems that the model decided in chapter three, which is more accurate for values below nominal point, was the correct one.

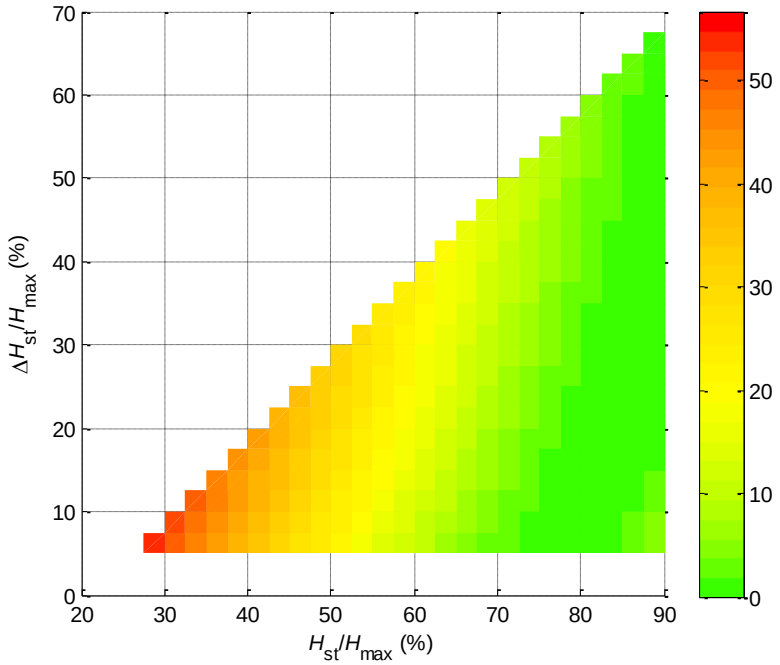

Figure 5.3 Best constant speed compared to nominal rotational speed of 1450 rpm (%).

Differences between the speed ramp and the best constant speed control methods are shown in figure 5.4. As can be seen speed ramp provides up to 15 % points more saved energy when there is static head variation of over 0.6. With $\Delta H_{st}/H_{max}$ being less than 0.1 there is little to no difference in energy consumption.

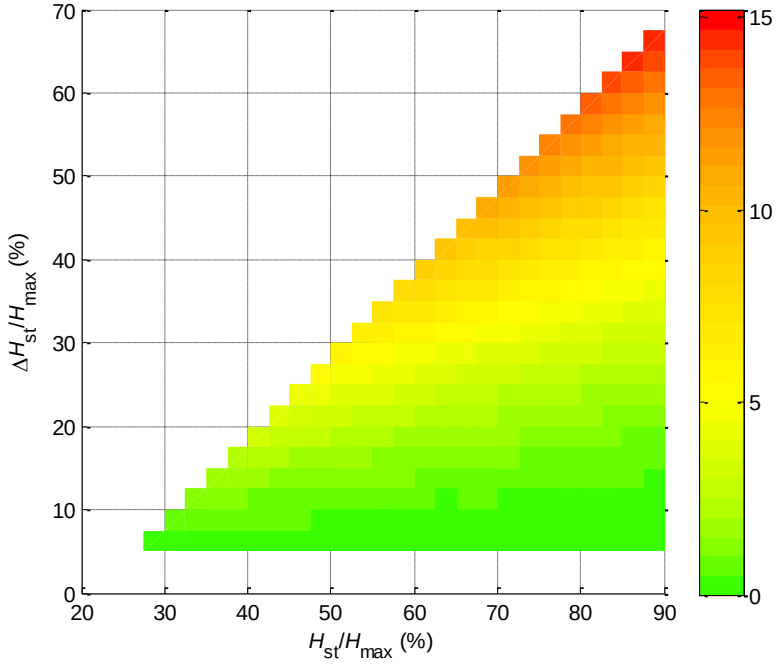

Figure 5.4 Speed ramp compared to the best constant speed (% point).

5.2 The effect of *k* on system's saving potential

Figure 5.5 shows how much potential energy savings are affected when systems friction factor has changed. Friction factors that are used are the base simulation value k_{base} 0.0149 (ms^2/l^2), half of the base value and double the base value. In the first column there is saving potential calculated by using the best constant speed for the process. In the second column the speed ramp has been used. In the third column difference between saving potential of these two control methods is presented in % points. As friction factor increases, saving potential decreases. This means that operation region where constant speed of 1450 rpm can be used efficiently is achieved with lower static head amount in the case of friction factor being $2*k_{base}$. With reduction of the relative static head amount, difference between these control methods and general saving potential increases.

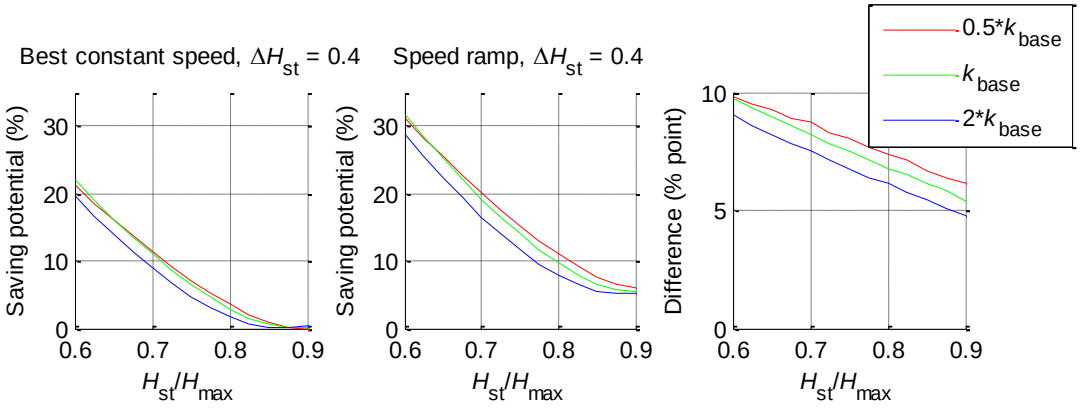

Figure 5.5 Different friction factors for variable speed control methods.

Figure 5.6 has expanded this analysis to two other static head variation values. First row contains same images as does figure 5.5. The second and the third row contain images with reduced static head variation. As already seen in figure 5.1, reduction of static head variation $\Delta H_{st}/H_{max}$ means that the system has less potential energy savings when utilizing variable speed control methods; reducing static head variation brings differences between these two control methods to less than 1 % when the variation is 0.1 or less.

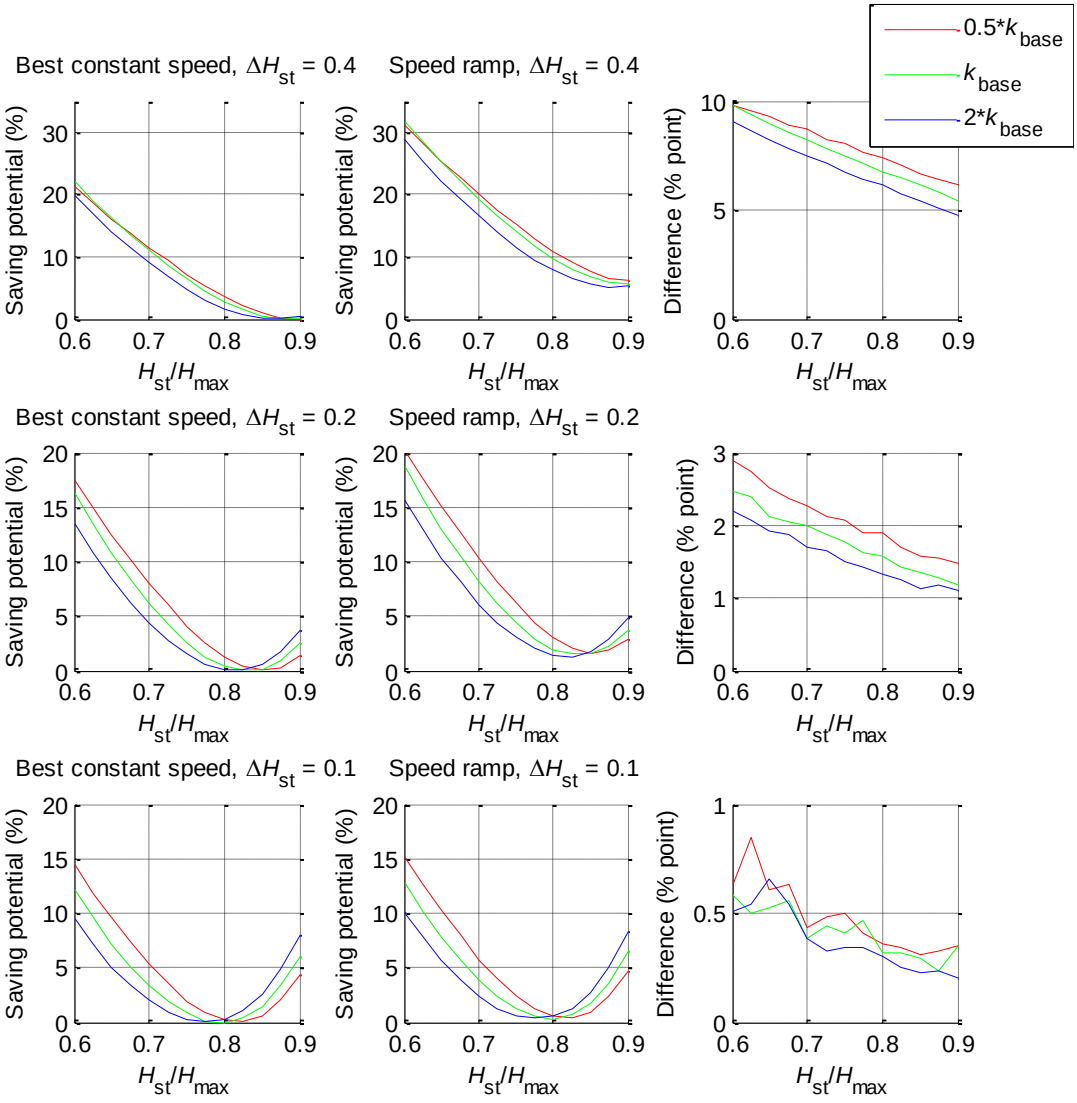

Figure 5.6 Different friction factors and various static head differences with both control methods.

Looking at figures 5.1 and 5.6 it appears that the amount of static head is the most dominant factor when determining the amount of saving potential in a system. Static head variation mostly affects the effectiveness of the chosen flow control method. There is possibly over 10 % point difference in saving potential between the two methods used in this thesis. Friction factor *k* seems to have the least amount of impact on saving potential out of these three parameters. To ensure this, further study would be required with different amounts of friction in the system.

5.3 Case Pietarsaari

Master's thesis about energy consumption in wastewater pumping had a case study showing that the main wastewater pumping station in Pietarsaari could have potentially up to 40

% less energy consumption with a proper constant speed (Ruuskanen, 2007). This is a prime example of reservoir pumping. Since there was some static head variation included it is now estimated how much more a proper speed ramp could provide energy savings.

In this pumping station static head could raise from 2 meters up to 5 meters while single pump could provide up to 18 meters of head with nominal speed of 1460 rpm. This would mean static head variation of 17 % and static head amount of 28 % in figures above. This region in figure 5.3 has saving potential of slightly over 40 % which is close to the value calculated in the master's thesis. By looking at this region in figure 5.4 there would be about 3 % point difference between speed ramp and the best constant speed.

From figure 5.7 friction factor can be calculated using information from the shown system with equation (2.1). Resulting friction factor (0.000134 ms^2/l^2) is smaller than value used in graph simulation. Because of this, as shown in figure 5.6, the resulting saving potential will actually be higher than 3 % points. Final estimated saving potential difference based on figures 5.4 and 5.6 is 5 %.

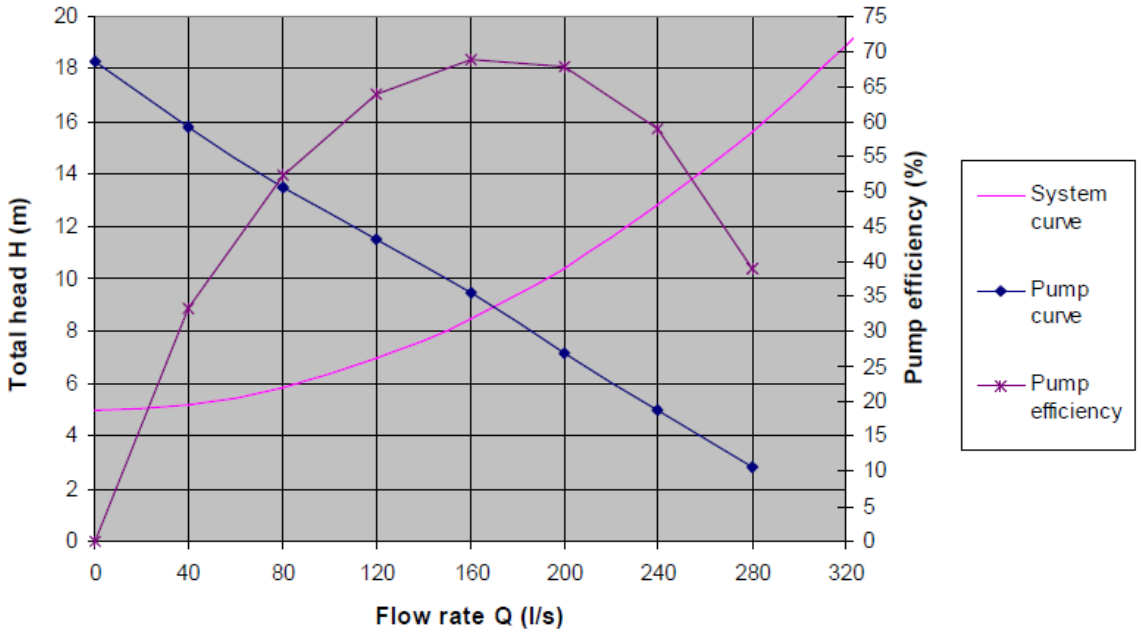

Figure 5.7 System, pump and efficiency curve for a pump in Pietarsaari (Ruuskanen, 2007).

Applying the same principles that were introduced in chapter four to calculate saving potential, there is a difference of 3 % points between the two variable speed control methods.

5.4 Case Heimosilta

In 2013, Lappeenrata University of Technology (LUT) conducted research on a local wastewater pumping station. This station already used speed ramp as a flow control method and it was studied can it be optimized better (Ahonen & Koponen, 2014).

In this pumping station, static head was 13.5 meters at maximum with variation of 0.65 meters. Maximum head for the pump was 35.5 meters. This results in static head amount of 38 % and static head variation $\Delta H_{st}/H_{max}$ to be 2 %. Friction factor was calculated to be 0,00048 ms^2/l^2. There is not much of a difference in saving potential between the speed ramp and the best constant speed with variation being less than 10 %.

By looking at the figure 5.2, estimated saving potential would be 35 %. However from measured values from the research it was calculated that the saving potential with the current speed ramp was 17 % and it would rise to 18 % with even better optimization. Calculating saving potential with methods in chapter four resulted in saving potential of 18.3 %. It appears that while the calculating methods yield accurate results, the graphs are not applicable in every scenario. This should be expected as they are drawn from results given by a single pump in a specific system.

6. CONCLUSION

A lot of information about pumping systems and their efficiency is available. Usually systems are looked at individually and choosing the best methods to achieve energy efficiency requires experience and knowledge of the current system. There is still lack of easy-to-use methods to quickly judge which direction to take when some characteristics, like static head and its variation, are known. Further studying the subject of this thesis could provide the needed results.

The goal of this thesis was achieved to some degree. It gives general idea when finding the best constant speed is as good of an option as calculating range of speeds for the operation. It shows how decided system variables and flow control methods affect energy savings but there are still flaws. Since this information was concluded from one process with characteristics of one specific pump, further testing would be required to judge whether or not these graphs represent behavior of specific energy in other systems with different pumps.

In the case examples there is given estimation how much more could be saved. While in the case Pietarsaari graphs predicted results close to the calculated values this did not happen in case Heimosilta. For Heimosilta pumping station the estimated value from graphs was over 90 % higher than what the calculated value was. It seems that the graphs presented in this thesis can only be used for certain type of pumps.

REFERENCES

ABB Oy. 2012. *PumpSave user's manual.*

Ahonen, T. 2011. *Monitoring of centrifugal pump operation by a frequency converter*. Lappeenranta.

Ahonen, T., Koponen, J. 2014. *Saneerauksen onnistuminen Heimosillan jätevedenpumppaamolla.* Vesitalous 2/2014, 32–35.

Ahonen, T., Tamminen, J., Viholainen, J., Ahola, J., Koponen, J. 2014. *Energy Efficiency Optimizing Rotational Speed Reference Generation Method for Reservoir Pumping Applications.*
http://link.springer.com/article/10.1007%2Fs12053-014-9282-6

Bene, J. 2013. *Pump schedule optimization techniques for water distribution systems.* Oulu.

Europump, Hydraulic institute. 2004. *Variable speed pumping, a guide to successful applications.* London: Elsevier Advanced Technology.

Europump, Hydraulic Institute, the US Department of Energy's Office of Industrial Technologies. 2001. *Pump Life Cycle Costs: A Guide to LCC Analysis for Pumping Systems.*
https://www1.eere.energy.gov/manufacturing/tech_assistance/pdfs/pumplcc_1001.pdf

Ferman, R., Hardee R., Livoti, W. C., Pemberton, M., Tutterow, V., Walters, T. 2008. *Optimizing pumping systems, a guide for improved energy efficiency, reliability & profitability*. New Jersey: Pump systems matter, Hydraulic institute.

Ruuskanen, A. 2007. *Optimization of energy consumption in wastewater pumping.* Helsinki.

Shields, S. 2004. *Stan Shields on Centrifugal Pumps: Collected Articles from "World Pumps" Magazine.* London: Elsevier Advanced Technology.